Potential of mean force between identical charged nanoparticles immersed in a size-asymmetric monovalent electrolyte

Guillermo Iván Guerrero-García, Pedro González-Mozuelos, and Mónica Olvera de la Cruz

Citation: The Journal of Chemical Physics **135**, 164705 (2011); doi: 10.1063/1.3656763
View online: http://dx.doi.org/10.1063/1.3656763
View Table of Contents: http://scitation.aip.org/content/aip/journal/jcp/135/16?ver=pdfcov
Published by the AIP Publishing

Potential of mean force between identical charged nanoparticles immersed in a size-asymmetric monovalent electrolyte

Guillermo Iván Guerrero-García,[1] Pedro González-Mozuelos,[2] and Mónica Olvera de la Cruz[3,a)]
[1]*Department of Chemistry, Northwestern University, Evanston, Illinois 60208, USA*
[2]*Departamento de Física, Cinvestav del I. P. N., Av. Instituto Politécnico Nacional 2508, Distrito Federal, C. P. 07360, México*
[3]*Department of Materials Science and Engineering, Northwestern University, Evanston, Illinois 60208, USA*

(Received 22 August 2011; accepted 6 October 2011; published online 31 October 2011)

In a previous theoretical and simulation study [G. I. Guerrero-García, E. González-Tovar, and M. Olvera de la Cruz, Soft Matter **6**, 2056 (2010)], it has been shown that an asymmetric charge neutralization and electrostatic screening depending on the charge polarity of a single nanoparticle occurs in the presence of a size-asymmetric monovalent electrolyte. This effect should also impact the effective potential between two macroions suspended in such a solution. Thus, in this work we study the mean force and the potential of mean force between two identical charged nanoparticles immersed in a size-asymmetric monovalent electrolyte, showing that these results go beyond the standard description provided by the well-known Derjaguin-Landau-Verwey-Overbeek theory. To include consistently the ion-size effects, molecular dynamics (MD) simulations and liquid theory calculations are performed at the McMillan-Mayer level of description in which the solvent is taken into account implicitly as a background continuum with the suitable dielectric constant. Long-range electrostatic interactions are handled properly in the simulations via the well established Ewald sums method and the pre-averaged Ewald sums approach, originally proposed for homogeneous ionic fluids. An asymmetric behavior with respect to the colloidal charge polarity is found for the effective interactions between two identical nanoparticles. In particular, short-range attractions are observed between two equally charged nanoparticles, even though our model does not include specific interactions; these attractions are greatly enhanced for anionic nanoparticles immersed in standard electrolytes where cations are smaller than anions. Practical implications of some of the presented results are also briefly discussed. A good accord between the standard Ewald method and the pre-averaged Ewald approach is attained, despite the fact that the ionic system studied here is certainly inhomogeneous. In general, good agreement between the liquid theory approach and MD simulations is also found. © *2011 American Institute of Physics*. [doi:10.1063/1.3656763]

I. INTRODUCTION

The study of intermolecular forces among charged colloids in aqueous media is a topic of great relevance in physical chemistry due to the vast number of possible technological applications.[1–3] The net attractive or repulsive character of such interactions determines the microscopic architecture and the relevant macroscopic properties depending on the colloidal stability. One of the theoretical cornerstones that has allowed important advances in the past century is the well known Derjaguin-Landau-Verwey-Overbeek (DLVO) theory, which relies on the Poisson-Boltzmann equation for point-ions. The applicability of this theory, however, is usually limited to low colloidal charges and diluted ionic systems. In fact, interesting phenomenology such as reversal of the electrophoretic mobility,[4,5] charge inversion,[6,7] and like-charge attraction in the presence of multivalent ions[8,9] cannot be predicted within this theoretical framework.

As it has been suggested by several authors, the ion-correlations neglected in the classical Poisson-Boltzmann theory may play a fundamental role in the description of the electrical double layer around charged colloidal particles in aqueous solutions,[10–14] and consequently affect the effective interactions among these particles. For example, Monte Carlo studies have shown that the potential of mean force (PMF) between two identical macroions immersed in a charge-asymmetric (2:1 or 1:2) supporting electrolyte of equal-sized ions behaves differently, at a given ionic strength, depending on the magnitude of the counterion valence.[15] On the other hand, a previous study demonstrated that if the solvent is taken into account explicitly, a charged-asymmetric behavior is also observed in the renormalized charge of a model nanoparticle immersed in a monovalent supporting electrolyte.[16] This characteristic, originated on the different degrees of ionic hydration, can be included in a coarse-grained model at the McMillan-Mayer level of description by considering different effective ionic diameters that mirror those hydration effects for each ionic species. Such an approach has already been implemented through Monte Carlo

a)Author to whom correspondence should be addressed. Electronic mail: m-olvera@northwestern.edu.

simulations of a size-asymmetric monovalent salt around a model charged nanoparticle, showing too an asymmetric charge neutralization and electrostatic screening which depends on the sign of the macroion charge.[17] One may surmise that these effects should also be manifest in the effective interactions between two identical charged nanoparticles.

Effective interactions among suspended charged nanoparticles are important for describing the thermodynamics of this type of solutions, including the phase diagrams that have been obtained experimentally,[18,19] numerically,[16,20] and via computer simulations.[21] The main aim of the current study is thus to determine these interactions when the macroions are immersed in a size-asymmetric monovalent electrolyte in order to examine the issues discussed above. Charge- and size-asymmetric bulk electrolytes have been extensively studied in the past.[22] Here, we consider a model system with three species of spherical particles: monovalent cations, monovalent anions, and charged nanoparticles. To isolate the effects induced by the size asymmetry between the cations and anions from other types of short-range attractions, the interactions among all these particles are modeled as the superposition of a soft repulsive core plus a Coulomb interaction between point charges situated at the center of each particle. The solvent is taken into account only through the value of the Bjerrum length in the electrostatic potential, that is, as a uniform background with a continuous dielectric constant. Since the anions have larger sizes than the cations in typical monovalent salts, the anions are assumed to be twice as large as the cations. The charge of the nanoparticles, the largest species in our model system, is varied within a wide range from negative to positive values. Molecular dynamics (MD) simulations and liquid theory calculations are then performed to evaluate the mean force and PMF between two identical nanoparticles. Both approaches show an analogous effect to that observed for a size-symmetric but charge-asymmetric supporting electrolyte:[15] the effective interaction between two cationic nanoparticles is markedly dissimilar from that between two anionic nanoparticles, even when their valence magnitudes are the same. For the systems studied in this work, however, this observation is attributable mainly to the ion-size differences between the counterions and coions, specially in their closest approach distances to the charged nanoparticles. In particular, the PMF between highly charged anionic nanoparticles displays an attractive well located at a distance consistent with electrostatic "bridging" by the monovalent cations. These results suggest that short-ranged attractions in monovalent size-asymmetric electrolytes are possible, even in the absence of specific interactions. Such attractions would have important consequences to bulk stability of nanoparticles and colloids and to their adsorption to air-liquid or liquid-liquid interfaces with dielectric discontinuities, since the adsorption of macroions to interfaces depends on the partition of ions in the bulk,[23,24] and might modify protein adsorption and the Hofmeister series.

As an additional objective for the current work, we also test here the performance of two different approaches for dealing with long-range electrostatic interactions within MD simulations. Computer simulations of systems with Coulomb potentials are not straightforward because simple truncation schemes for these long-range interactions are inappropriate. A typical approach to overcome this issue is attained by using the classical Ewald sums technique, which is the standard protocol used in simulating ionic fluids.[25] In the best case scenario, however, this scheme scales as $O(N^{3/2})$, which limits considerably the number of particles that can be simulated. Thus, more sophisticated computational approaches of complexity $O(N\log N)$ (Ref. 26) have been considered in the past for the study of large ionic systems. An alternative avenue to face this problem could be attained by using graphics processing units (GPUs), which have shown an excellent performance in simulating systems with short-range interactions.[27,28] In a previous work, the pre-averaged (P-A) Ewald sums method,[29] originally proposed for studying homogeneous ionic systems, was implemented in GPUs.[30] Given the good performance and excellent agreement with the standard Ewald summation method shown in that instance, we wondered if such scheme would be adequate to perform simulations of inhomogeneous systems, viewed as perturbations of the homogeneous ones. Thus, we also test here the performance of the P-A Ewald sums against the standard Ewald summation for a inhomogeneous systems constituted by two fixed nanoparticles immersed in a size-asymmetric monovalent electrolyte.

The layout of this paper is as follows. In Sec. II, we describe the details of the model system and provide an overview of the computer simulation and liquid theory approaches. Section III presents the results and discussion of this study. We finish with some concluding remarks in Sec. IV.

II. MODEL, SIMULATIONS, AND THEORY

The model system studied here is constituted by two identical nanoparticles immersed in a monovalent size-asymmetric electrolyte with the solvent considered as a uniform dielectric background; we are thus considering such a system at the McMillan-Mayer level of description. In this approach, the ionic species are considered as charged soft-core spheres of effective diameter d_i with point charges $z_i e$ embedded in their centers, where z_i is the valence of a charged particle of species i and e corresponds to the proton charge. Thus, the repulsive core potential between a particle of species i and a particle of species j separated at a distance r is modeled using a shifted-truncated Lennard-Jones potential:

$$\beta u_{ij}^{rc}(r) = \begin{cases} \infty, & \text{for } r \le \Delta_{ij} \\ 4\left[\left(\frac{\sigma}{r-\Delta_{ij}}\right)^{12} - \left(\frac{\sigma}{r-\Delta_{ij}}\right)^{6}\right] + 1, & \text{for } \Delta_{ij} < r < \Delta_{ij} + 2^{1/6}\sigma \\ 0, & \text{for } r \ge \Delta_{ij} + 2^{1/6}\sigma, \end{cases} \quad (1)$$

TABLE I. Parameter values used in the MD simulations and the integral equation approach.

Valence of each nanoparticle	z_M
Valence of cations	$z_+ = +1$
Valence of anions	$z_- = -1$
Diameter of each nanoparticle	$d_M = 3.0$ nm
Diameter of cations	$d_+ = 0.425$ nm
Diameter of anions	$d_- = 2d_+$
Molar density of cations	$\rho_+ = 1$M
Molar density of anions	$\rho_- = 1$M
Dielectric constant	$\epsilon = 78.5$
Temperature	$T = 298$ K
Bjerrum length	$l_b = 0.714$ nm

where $\beta \equiv (k_B T)^{-1}$, k_B and T being, respectively, the Boltzmann constant and the temperature of the system, and $\Delta_{ij} = (d_i + d_j)/2 - \sigma$ is the hard-core diameter. The parameter σ is then set equal to the diameter of the smallest ionic species, which in our case are the monovalent cations, so that $\sigma = d_+$. These parameters were selected in order to have the same "hardness" between all charged particles, so $\beta u_{ij}^{rc}((d_i + d_j)/2) = 1$, and the form of the potential guarantees a soft continuous repulsion beyond the inner core, that is, for $r > \Delta_{ij}$.

To this repulsive core should be added the pair potential representing the electrostatic interaction between an ion of species i and an ion of species j, which is expressed by

$$\beta u_{ij}^{el}(r) = \frac{l_b}{r} z_i z_j, \tag{2}$$

where $l_b = e^2/(4\pi\epsilon_0\epsilon k_B T)$ is the corresponding Bjerrum length, ϵ_0 is the vacuum permittivity, and ϵ is the dielectric constant of the background medium. At the McMillan-Mayer level of description considered here, as stated above, all the solvent effects are then taken into account via this continuum dielectric medium that fills the whole space. For an aqueous solution $\epsilon \approx 80$.

While the focus of the present work is in the mean force and the PMF between two equally charged nanoparticles, similar parameter values, which are summarized in Table I, have already been used in a previous study of the distribution of size-asymmetric monovalent ions around a single charged nanoparticle, though with hard-sphere cores instead of the soft-sphere cores considered here.[17] The range of valence values for the nanoparticles considered in the present study goes from $z_M = -54$ up to $z_M = +54$, including $z_M = 0$.

Coulomb interactions are long-ranged, so special techniques are required to take them into account properly. The usual approach to handle the electrostatic interactions with the distant particles images in computer simulations is via the standard Ewald sums method, which is the customary technique to study ionic fluids nowadays. Nonetheless, in a previous work[30] the P-A Ewald sums approach proposed by Yakub *et al.*[29] was implemented in GPUs and showed to yield results comparable to those from the standard Ewald sums method. Interestingly, it has been proposed very recently that the P-A Ewald method and the Wolf method[31] are both particular limits of the zero-dipole summation method,[32] which is intended to prevent nonzero-charge and nonzero-dipole contributions arising spuriously from a simple truncation scheme. On the other hand, the P-A Ewald approach is best suited to study homogeneous or isotropic ionic systems, and also has the advantage that its GPU implementation can be much faster than an optimized central processing unit version of Ewald sums method for a small to a sizable number of particles ($\sim 10^5$).[30] We wondered if such method could be used too in the study of inhomogeneous systems, so in the present work we test its performance using the molecular dynamics HOOMD program[27,33] versus the classical Ewald sums scheme using the LAMMPS package.[34,35]

A cubic simulation cell with periodic boundary conditions is used here for the MD simulations. Two identical nanoparticles were located at fixed positions along one diagonal of the cubic simulation box, symmetrically with respect to the center of the cell, while surrounded by the freely moving monovalent ions contained within the same cell. The charged particles in the simulation box fulfill the electroneutrality condition,

$$2z_M + z_c N_c + z_+ N_+ + z_- N_- = 0, \tag{3}$$

where N_+ and N_- are, respectively, the number of bulk monovalent cations and anions, while z_c and N_c are the corresponding valence and number of monovalent counterions added to compensate the charge of the two nanoparticles (of course, in the case of anionic nanoparticles the added counterions are small cations, whereas for cationic nanoparticles the added counterions are large anions, that is, $z_c = z_+$ for $z_M < 0$ and $z_c = z_-$ for $z_M > 0$, etc.). The MD simulations were performed in the NVT ensemble via a Nosé-Hoover thermostat[36,37] at a reduced temperature $T' = k_B T/\epsilon = 1$, where $\epsilon = k_B T$ is the thermal energy. In Lennard-Jones reduced units, the distance, mass, and energy were rescaled regarding the mass and diameter of the smallest ionic species and the thermal energy, that is, $m_i' = m_i/m_+$, $x' = x/d_+$, and $u' = u/\epsilon$. The time step used was 0.005τ, where $\tau = \sqrt{m_+' d_+'^2/\varepsilon'}$ is the reduced Lennard-Jones unit of time. The total number of ions $N = N_+ + N_- + N_c$ used in a typical simulation was around 2000. One million of MD time steps were used to thermalize the system. The total repulsive core and electrostatic forces acting over each nanoparticle where sampled each 10 MD time steps (in a compromise between efficiency and reduction of time correlations), and between 14×10^6 to 24×10^6 of MD time steps were performed to calculate the time average of the forces.

At a given instant, the net force exerted over one nanoparticle, labeled as A and located at the position $\vec{r}_A$, is the sum of the direct force exerted by the other nanoparticle, labeled as B and located at $\vec{r}_B$, plus the sum of the forces exerted by each one of the mobile ions, located, respectively, at the positions $\vec{r}_i^{(\gamma)}$, where $\gamma = +, -$ and $i = 1, 2, ..., N_\gamma$. Thus, it is a superposition of the repulsive core and electrostatic components,

$$\vec{F}^A(\vec{r}_A) = \vec{F}_{rc}^A(\vec{r}_A) + \vec{F}_{el}^A(\vec{r}_A), \tag{4}$$

given by

$$\vec{F}^{A}_{xx}(\vec{r}_A) = -\vec{\nabla}_A u^{xx}_{MM}(|\vec{r}_A - \vec{r}_B|) - \sum_{\gamma=+,-}\sum_{i=1}^{N_\gamma} \vec{\nabla}_A u^{xx}_{M\gamma}\left(|\vec{r}_A - \vec{r}_i^{(\gamma)}|\right), \quad (5)$$

where xx stands for rc or el, and $\vec{\nabla}_A$ denotes the gradient with respect to $\vec{r}_A$. Due to the symmetry of the system, the ensemble average of the net force over the nanoparticle A must lie in the direction of $\vec{r}_A - \vec{r}_B$, and moreover, be a function only of the separation distance between the centers of the two nanoparticles $r = |\vec{r}_A - \vec{r}_B|$. Thus, after averaging over all the configurations, one obtains the corresponding magnitudes for the mean forces:

$$F(r) = F_{rc}(r) + F_{el}(r), \quad (6)$$

where

$$F_{xx}(r)\hat{r}_{AB} = \left\langle \vec{F}^{A}_{xx}(\vec{r}_A)\right\rangle, \quad (7)$$

with xx again standing for rc or el, while $\langle\cdots\rangle$ denotes time average in the MD simulations, and $\hat{r}_{AB}$ is the unit vector pointing in the direction from B to A. With these definitions, positive values of $F(r)$ correspond to repulsive mean forces between the nanoparticles, while negative values correspond to attractive mean forces, and the same applies to its components.

The PMF represents the work necessary to move one nanoparticle from infinite to a distance r with respect to the other nanoparticle, and can be calculated from the mean force by integrating it numerically,

$$W(r) = \int_r^\infty F(r)dr. \quad (8)$$

Thus, the PMF can then be written as the sum of the corresponding repulsive core and Coulomb components of this potential,

$$W(r) = W_{rc}(r) + W_{el}(r), \quad (9)$$

with

$$W_{xx}(r) = \int_r^\infty F_{xx}(r)dr, \quad (10)$$

where, once more, xx stands for rc or el.

The analogous results from the liquid theory approach are attained as follows. We start by solving the Ornstein-Zernike (OZ) equations,

$$h_{ij}(r_{12}) = c_{ij}(r_{12}) + \sum_{k=M,+,-} \rho_k \int d\vec{r}_3 c_{ik}(r_{13})h_{kj}(r_{32}), \quad (11)$$

for $i, j = M, +, -$, where $r_{mn} = |\vec{r}_m - \vec{r}_n|$, complemented with the hyper-netted chain (HNC) closure,

$$c_{ij}(r) = -\beta u_{ij}(r) + h_{ij}(r) - \ln(1 + h_{ij}(r)). \quad (12)$$

Thus, the inputs for this closed set of non-linear integral equations are the pair potentials $u_{ij}(r) = u^{rc}_{ij}(r) + u^{el}_{ij}(r)$, determined by Eqs. (1) and (2), and the bulk number densities ρ_i, whereas the outputs are the total and direct correlation functions $h_{ij}(r)$ and $c_{ij}(r)$, respectively. The method employed for the solution of this set of equations is based on the Ng prescription.[38] All our calculations were performed on an array of 2^{16} points with a lattice spacing of 0.002 nm. The OZ self-consistency and the Stillinger-Lovett first moment condition are converged to at least 1 part in 10^8. For the present study, we are considering the limit of infinite nanoparticle dilution, so $\rho_M = 0$. The relation,

$$\beta W(r) = -\ln(1 + h_{MM}(r)), \quad (13)$$

thus provides the corresponding total PMF, which, in this limit of infinite dilution, is equivalent to the effective pair potential between two nanoparticles.[39]

In addition, it is also useful to compare the $W_{el}(r)$ obtained from the computer simulations to the electrostatic component of the well-known DLVO potential, given by

$$\beta W_{\mathrm{DLVO}}(r) = \frac{l_b}{r}\frac{z_M^2 \exp(-\kappa_D(r - d_M))}{(1 + \kappa_D d_M/2)^2}, \quad (14)$$

where

$$\kappa_D = \sqrt{4\pi l_b(\rho_+ z_+^2 + \rho_- z_-^2)} \quad (15)$$

is the inverse Debye screening length.[40] Since this effective potential is the usual starting point in many studies of colloidal suspensions,[41,42] it is of great interest to test its strengths and limitations under the conditions considered here.

III. RESULTS AND DISCUSSION

We start our analysis of the mean forces and PMFs between two identical nanoparticles by comparing the case of neutral ($z_M = 0$) macroions immersed in our model size-asymmetric monovalent electrolyte against an identical system but with the electrostatic interactions turned off, that is, one in which $l_b = 0$ (physically corresponding to a system where all particles are uncharged, among other possibilities). The latter provides us with a baseline to quantify the contribution from the depletion forces due to the repulsive core interactions. The corresponding results for $\beta F(r)l_b$ and $\beta W(r)$ as a function of the separation distance r are presented in Figure 1. It is observed here that the mean forces and PMFs between the two neutral nanoparticles immersed in the size-asymmetric electrolyte are virtually the same for both cases, that is, for $l_b = 0.714$ nm and $l_b = 0$. This seems to imply that, for $z_M = 0$, the effects coming from the ionic electrostatic interactions are negligible in comparison to the excluded volume effects with regard to the correlations involving the nanoparticles. This is in agreement with a previous study of the electrical double layer around a single nanoparticle.[17] Hence, the short-range attraction illustrated by the first minimum in the PMF is due mainly to depletion forces operating when the nanoparticles are separated at a distance slightly larger than the "effective" hard-sphere contact distance $r \approx d_M \approx 7.06d_+$. This attraction decreases as the separation between the nanoparticles increases, and at some point the mean force becomes repulsive, which corresponds to the maximum in the PMF at $r \approx d_M + d_+$; at this separation distance there is just enough room to fit a small cation between the two nanoparticles. For larger separations, the damped oscillatory

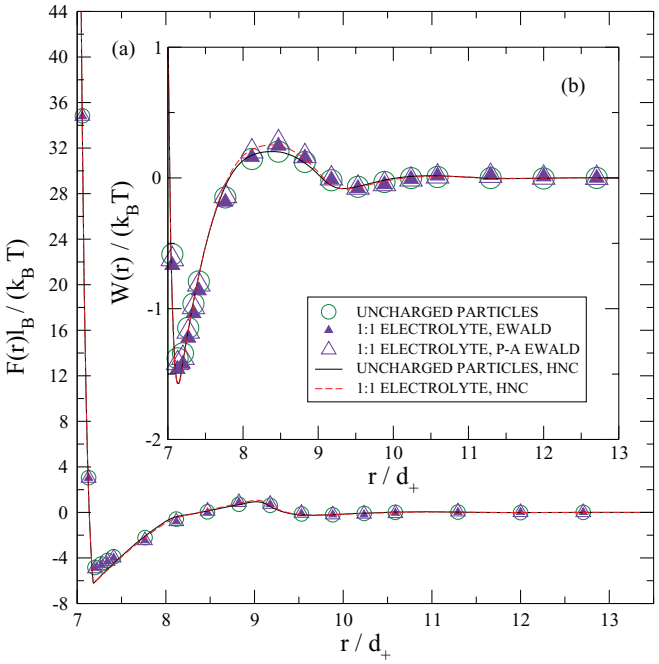

FIG. 1. Mean force (a) and potential of mean force (PMF) (b) between two neutral nanoparticles. The triangles correspond to MD results for $F(r)$ and $W(r)$ when the nanoparticles are immersed in a 1:1 size-asymmetric electrolyte at 1M. The data represented by filled and empty triangles are obtained, respectively, by using the standard Ewald method and the pre-averaged Ewald approach. The empty circles represent MD results for a system with the same parameters for d_M, d_+, d_-, and $\rho_+ = \rho_-$, but with $l_b = 0$ instead of $l_b = 0.714$ nm. The lines show the corresponding HNC predictions of $F(r)$ and $W(r)$: dashed lines represent $l_b = 0.714$ nm and solid lines represent $l_b = 0$. Here, and in the rest of the figures, the numerical uncertainties are smaller than the size of the symbols.

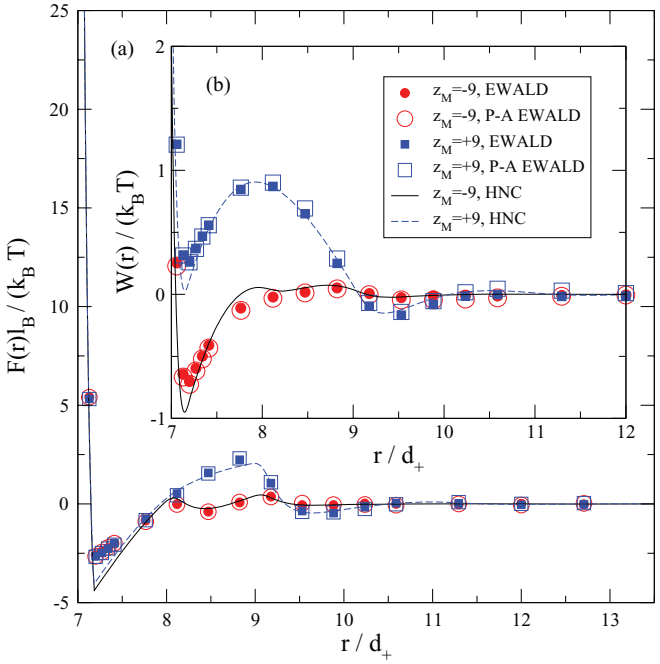

FIG. 2. Mean force (a) and PMF (b) between two identical charged nanoparticles immersed in a 1:1 size-asymmetric electrolyte at 1M. Circles and squares correspond, respectively, to MD results for $z_M = -9$ and $z_M = +9$. Filled and empty symbols represent simulation data obtained, respectively, with the standard Ewald method and the pre-averaged Ewald approach. Solid and dashed lines display, respectively, the corresponding HNC predictions for $z_M = -9$ and $z_M = +9$.

behavior typical of hard spheres systems is shown by $F(r)$ and $W(r)$. It is also clear that, under these circumstances, the HNC results show a very good agreement with the simulation data. The largest discrepancy is found at the contact distance $r = d_M$, where the liquid theory approach seems to slightly overestimate the attraction. In addition, for $l_b = 0.714$ nm, the simulation predictions obtained with the P-A Ewald approach closely match those attained with the standard Ewald summation method.

More noticeable differences between the theoretical and simulation calculations exist for situations involving charged nanoparticles ($l_b = 0.714$ nm from now on). Figure 2 illustrates the results corresponding to two cases: $z_M = -9$ and $z_M = +9$. As can be appreciated at once, the sign of the nanoparticle valence plays a crucial role in the determination of the effective interaction between two identical charged nanoparticles, even though the magnitude of these valences is the same in both cases. This charge-asymmetric behavior for the effective interactions between the two identical nanoparticles is, of course, a direct consequence of the size-asymmetry in the supporting electrolyte, which indeed induces different ionic distributions around each macroion.[17] In each case, the HNC results and the MD data show again the same general behavior, with the theoretical approach once more overestimating the attraction near the contact distance $r \approx d_M$. This feature is perhaps more easily observed in the corresponding PMFs, shown in the inset, where the difference between the depths of the attractive wells around $r \approx d_M$ are more conspicuous, clearly indicating that it is harder for cationic nanoparticles to reach contact. Nonetheless, there is also a secondary minimum in the PMF for $z_M = +9$ at $r \approx 9.5d_+$ that indicates a slight trend for nanoparticle binding at that separation distance.

To elucidate the origin of the features just discussed, we present separately in Figure 3 the respective repulsive core and Coulomb components of the PMFs shown in the previous figure. The first general observation here is that the results attained from the P-A Ewald approach turn out to be practically identical to those obtained from the classical Ewald summation, even at the level of each one of these components, which clearly validates the use of the P-A Ewald sums scheme for the present conditions. With regard to the charge-asymmetric behavior, the differences between the two cases are indeed mirrored in the behavior of these components. For the case of negatively charged nanoparticles (Figure 3(a)), $W_{rc}(r)$ has an attractive well at $r \approx d_M$, that is larger in magnitude than $W_{el}(r)$ at $r \approx d_M$, which is basically repulsive in this region. The result is the net attraction displayed by $W(r)$ at contact for $z_M = -9$. In contrast, for the positively charged nanoparticles (Figure 3(b)), the attractive well of $W_{rc}(r)$ at $r \approx d_M$ is certainly of smaller magnitude that the repulsive $W_{el}(r)$ at the same separation distance, thus yielding for $z_M = +9$ a less favorable attractive well at contact for the total $W(r)$. It is also interesting to notice that $W_{rc}(r)$ seems to have wider oscillations for cationic nanoparticles, with a more clearly defined secondary minimum at $r \approx 9.5d_+$, than for

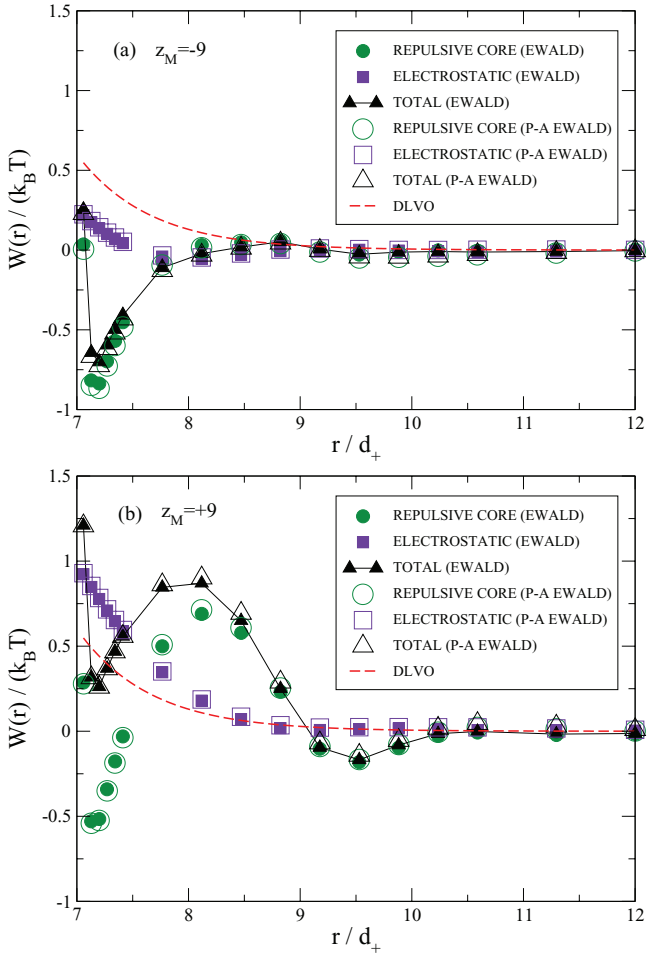

FIG. 3. Contributions to the PMF between two identical charged nanoparticles immersed in a 1:1 size-asymmetric electrolyte at 1M. The nanoparticle valence is $z_M = -9$ in (a) and $z_M = +9$ in (b). Triangles, circles, and squares correspond, respectively, to $W(r)$ and its repulsive core and electrostatic contributions obtained via MD simulations. Filled and empty symbols represent, respectively, the data obtained using the standard Ewald method and the pre-averaged Ewald approach. Lines joining symbols are intended as an eye-guide.

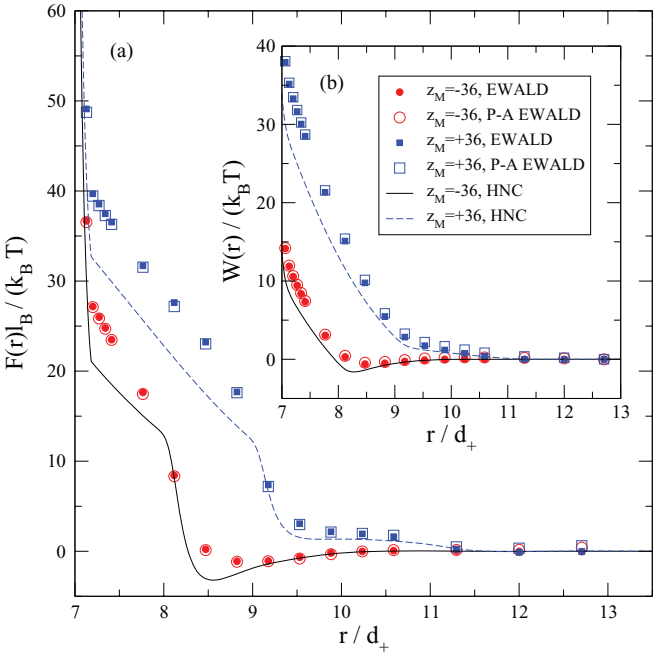

FIG. 4. Mean force (a) and PMF (b) between two identical charged nanoparticles immersed in a 1:1 size-asymmetric electrolyte at 1M. Circles and squares correspond, respectively, to MD results for $z_M = -36$ and $z_M = +36$. Filled and empty symbols represent simulation data obtained, respectively, with the standard Ewald method and the pre-averaged Ewald approach. Solid and dashed lines display, respectively, the corresponding HNC predictions for $z_M = -36$ and $z_M = +36$.

anionic ones. Moreover, the position of this secondary minimum roughly corresponds to a separation distance between the two nanoparticles at which an anion fits tightly in the middle: $r \approx d_M + d_-$. With regard to $W_{el}(r)$, on the other hand, for the case corresponding to $z_M = +9$ it seems to be almost monotonously repulsive, whereas for the case corresponding to $z_M = -9$ it shows and oscillatory behavior with an almost negligible minimum at $r \approx 8.1d_+$, which roughly corresponds to the situation of two nanoparticles with a cation squeezed in between ($r \approx d_M + d_+$). This electrostatic bridging effect thus seems to play a rather small role, for this instance, in the overall behavior of the PMFs; however, as suggested below, it may be more relevant at larger magnitudes of the nanoparticle valence. For comparison purposes, the corresponding DLVO predictions are also plotted in Figures 3(a) and 3(b). For anionic (cationic) nanoparticles, it is found that DLVO clearly overestimates (underestimates) the $W_{el}(r)$ obtained from the computer simulations. The discrepancies between $W_{\mathrm{DLVO}}(r)$ and the simulation results for $W(r)$ illustrate the relevance of including consistently the ionic sizes in an approach beyond the classical Poisson-Boltzmann picture of point-like ions.

The effects of a larger magnitude of the nanoparticle charge are illustrated in Figure 4 where the mean forces and the matching PMFs for $z_M = -36$ and $z_M = +36$ are plotted. As for the previous cases, the agreement between the P-A Ewald approach and the standard Ewald method is very good with regard to the MD data, but the discrepancy of these with the liquid theory results is now more conspicuous; overall, the HNC approach seems to underestimate the repulsion between the two identical nanoparticles. Nonetheless, the general behavior predicted by both approaches is quite similar, in particular with regard to the charge-asymmetry effects: the effective interaction between cationic nanoparticles is significantly more repulsive than the one between anionic nanoparticles. Moreover, in the second case there is even an attractive well for $W(r)$ (rather shallow and located at around $r \approx 8.6d_+$ according to the simulation data, slightly deeper and closer to the origin according to the liquid theory results), with the ensuing effect on the respective $F(r)$.

Further insights into the source of the effects discussed above is attained by looking at the corresponding contributions from the repulsive core and electrostatic constituents of the PMFs, which are plotted in Figure 5. Again, even at the level of each one of these components the results from the P-A Ewald approach are virtually indistinguishable from those attained with the standard Ewald method, justifying once more the use of the more efficient P-A Ewald sums scheme in GPUs. Likewise, the charge-asymmetric behavior of the effective interactions is also reflected in each one of these contributions. In the case of negatively charged nanoparticles, illustrated in Figure 5(a), it is observed that near the contact

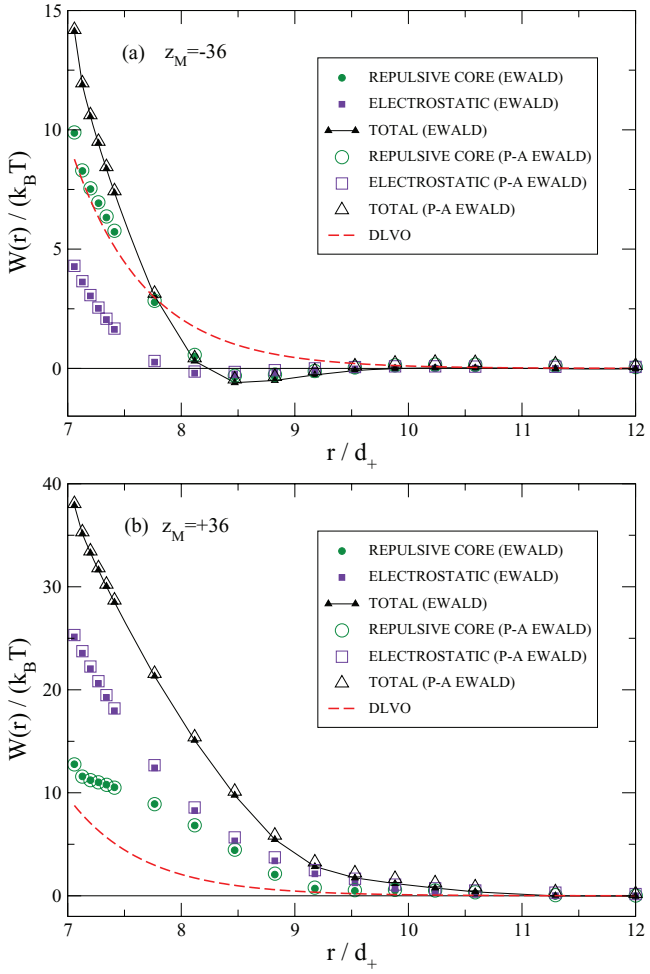

FIG. 5. Contributions to the PMF between two identical charged nanoparticles immersed in a 1:1 size-asymmetric electrolyte at 1M. The nanoparticle valence is $z_M = -36$ in (a) and $z_M = +36$ in (b). Triangles, circles, and squares correspond, respectively, to $W(r)$ and its repulsive core and electrostatic contributions obtained via MD simulations. Filled and empty symbols represent, respectively, the data obtained using the standard Ewald method and the pre-averaged Ewald approach. Lines joining symbols are intended as an eye-guide.

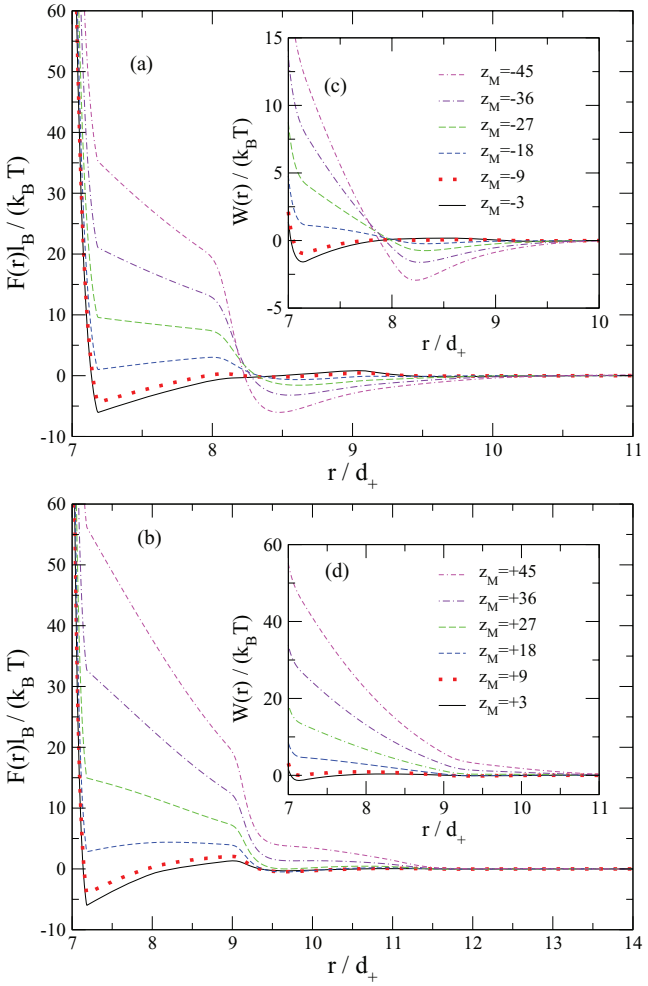

FIG. 6. Liquid theory predictions using the HNC closure for the mean force and the PMF between two identical nanoparticles immersed in a 1:1 size-asymmetric electrolyte at 1M. Panes (a) and (c) correspond to anionic nanoparticles, whereas panes (b) and (d) correspond to cationic nanoparticles. Solid, dotted, short-dashed, long-dashed, dotted-dashed and dotted-double-dashed lines represent the data for $|z_M| = 3, 9, 18, 27, 36, 45$, respectively.

distance $r \approx d_M$ both the $W_{rc}(r)$ and $W_{el}(r)$ are repulsive, the first being clearly larger than the second. Both contributions, however, display similar minima at the separation distance $r \gtrsim d_M + d_+$ for which there is just enough room to accommodate one cation in between the nanoparticles. This again suggests an electrostatic bridging between the two anionic nanoparticles, now somewhat larger than the one observed in Figure 3(a) since the presence of a counterion amid them is more electrostatically favorably. Figure 5(b), on the other hand, shows that for positively charged nanoparticles both constituents of the PMF are repulsive not only near the contact distance $r \approx d_M$, but also for all values of r. Furthermore, the electrostatic contribution in the case of cationic nanoparticles is larger than the repulsive core one for the whole range of separation distances.

Since the HNC results provide a qualitatively good and relatively accurate description of the effective interactions gathered from the computer simulation runs, it seems sensible to use the computationally less demanding liquid theory approach for a more extensive exploration of the effects of the nanoparticle charge. This analysis is displayed in Figure 6, where the mean forces and the PMFs pertaining to different values of the nanoparticle valence are plotted. It is immediately clear that, regardless of the sign of z_M, for low values of its magnitude an attractive effective interaction, due mainly to depletion forces, appears near the contact distance $r \approx d_M$. As the magnitude of z_M increases, this attractive interaction is overcome by the electrostatic repulsion between the identical nanoparticles, until it disappears completely for large enough values of $|z_M|$. As commented above, at this point the net repulsion at contact is evidently stronger between cationic nanoparticles than between anionic ones. The charge-asymmetric behavior of $W(r)$ is, however, even more marked beyond this contact region. For the case of anionic nanoparticles, illustrated in Figures 6(a) and 6(c), a secondary minimum in $W(r)$, situated around $r = 8.5d_+ \approx d_M + d_+$ and seemingly induced by the bridging role of the small cations, develops and deepens as the magnitude of z_M goes up, in accord to the results of the previous figures. Contrastingly, for

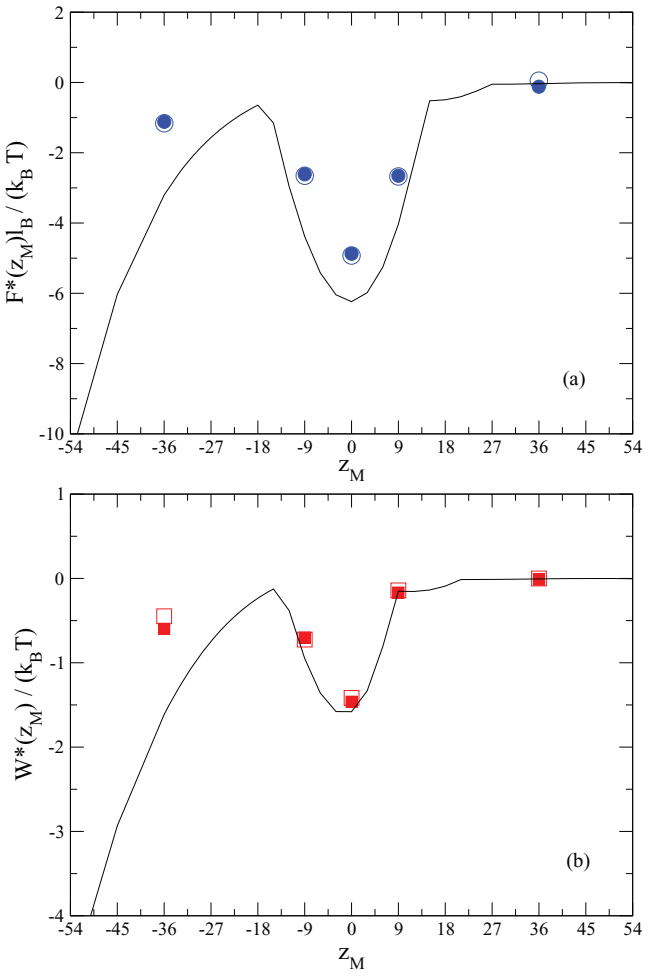

FIG. 7. Maximum reversed value of the mean force, F^*, and maximum reversed value of the PMF, W^*, between two identical nanoparticles immersed in a 1:1 size-asymmetric electrolyte at 1M as a function of the nanoparticle valence z_M. Symbols and solid lines correspond, respectively, to MD data and HNC results. Filled and empty symbols correspond to calculations using the standard Ewald method and the pre-averaged Ewald approach, respectively.

the case of cationic nanoparticles, illustrated in Figures 6(b) and 6(d), once the contact attraction is overwhelmed by the electrostatic repulsion, the effective interaction between identical nanoparticles becomes repulsive for all separation distances.

The relative importance of these attractive forces can be better appreciated by looking at the data presented in Figure 7, where the minimum values of the mean force and PMF between two identical nanoparticles, denoted by F^* and W^*, respectively, are plotted as a function of the nanoparticle valence ($F^* \leq F(r)$ and $W^* \leq W(r)$ for all separation distances r). The continuous lines represent the HNC results, and the symbols report the computer simulation data. The corresponding values for the electrostatic component of the DLVO potential, derived under the assumption of point-like ions in the supporting electrolyte, are necessarily zero since this component is always repulsive. As seen in Figure 7, around the point of zero nanoparticle charge the effective interactions display an attraction which is related mainly to depletion forces. As the magnitude of the nanoparticle valence increases, this contact attraction decreases due to the augmented direct electrostatic repulsion. In the case of cationic nanoparticles (surrounded by large counterions) this diminishment is monotonic, whereas for anionic nanoparticles (covered by small counterions) the effective interaction becomes again more attractive as the magnitude of the nanoparticle charge augments. This last observation is consistent with recent theoretical and simulation studies which show that, for a single charged nanoparticle immersed in a size-asymmetric monovalent electrolyte under similar conditions to the present study, charge reversal in the presence of small counterions grows monotonically as a function of the colloidal valence for high surface charge densities, whereas for large counterions the charge reversal observed near the point of zero charge disappears at larger colloidal charges.[43]

IV. CONCLUDING REMARKS

This work presents an study of the effective interactions between two identical spherical macroions immersed in a 1:1 ionic solution at a 1M concentration, focusing in particular on the effects induced by the asymmetry of ionic sizes in the supporting electrolyte. This is done by considering a model system in which the effective diameter of the anions is twice that of the cations. The consistent inclusion of ionic size-asymmetry (standing for the different hydration shell radii) provides a simpler approach to some of the mechanisms involved in more sophisticated but resource-expensive explicit solvent models. The main consequence of this size-asymmetry is a corresponding charge-asymmetric behavior of the effective macroion-macroion interactions: the PMF between two anionic nanoparticles, for example, is markedly distinct to the PMF between two cationic nanoparticles, even though the magnitude of the charge of these macroions is the same in both cases. This is indeed explained by the differences in the arrangement of the monovalent ions around the charged nanoparticles. As was described previously,[17] the local density of counterions in the vicinity of the nanoparticles is, as expected, larger than the corresponding density of coions. For cationic nanoparticles, however, these counterions are located farther away than for anionic ones, thus shifting the corresponding charge screening to larger distances from the surface of the macroion. For high surface charge densities, charge reversal can be significantly enhanced by small counterions, and even disappear for large counterions.[43] This charge-asymmetric arrangement of counterions and coions all over the charged nanoparticles also plays a determining role in the depletion forces induced by the short-range repulsive interactions among all these components, as illustrated by the respective plots of $W_{rc}(r)$ in Figures 3 and 5. The nature of these depletion forces is illuminated by the analysis of the effective interactions between neutral nanoparticles, which turn out to be practically equivalent to those obtained under the same general conditions but with all the electrostatic interactions turned off (i. e., setting $l_b = 0$).

A particularly interesting feature of the charge-asymmetric behavior of the effective nanoparticle-nanoparticle interactions is the emergence of attractive forces between highly charged anionic nanoparticles that operate at separations beyond the effective contact distance. A previous

Monte Carlo study demonstrated that an analogous charge-asymmetric behavior is also observable for the PMFs between two identical macroions immersed in a 2:1 or 1:2 size-symmetric electrolyte.[15] In that case, the presence of divalent counterions was critical to the onset of the effective electrostatic bridging. For the conditions considered in this work, however, the medium-range attraction is induced by the ionic size-asymmetry and has a depletion-like component besides the bare electrostatic bridging contribution. Thus, in the case of highly charged anionic nanoparticles the (smaller) counterions are adsorbed so strongly to each macroion that the configuration in which both share a layer of these counterions seems to be favorable despite the direct Coulomb repulsion between the nanoparticles. In contrast, the very strong repulsion observed between highly charged cationic nanoparticles indicates that the presence of large counterions completely inhibits any close binding among the macroions. This suggests that size-asymmetric monovalent electrolytes could enhance the solubility of strongly screened nanoparticles (at small Debye lengths, for example), even if attractive van der Waals dispersion forces are present, as it has been observed experimentally.[19] All the effects commented here are neglected by the widely used DLVO potential, which predicts the same behavior for the effective interaction between any two identical charged nanoparticles, regardless of their charge polarity, as long as they are immersed in the same supporting electrolyte. A similar situation is expected from other more sophisticated mean-field approaches that still rely on Yukawa-like linearized solutions of the Poisson-Boltzman theory,[44] thus emphasizing the relevance of taking into account the ion-ion correlations properly. Nonetheless, as the ionic concentration decreases the ionic correlations, and hence the ionic size asymmetry, become indeed less important, so for sufficiently diluted solutions the above phenomenology is expected to disappear. In such scenario, a mean-field description using point-like ions would be appropriate.

A deeper understanding of the type of mechanisms discussed here should allow the possibility of fine-tuning the physicochemical properties and the phase stability of complex fluids with the aim of enhancing their industrial and biomedical applications. Since the liquid theory approach also provides a sensible close description of these effects, it is reasonable to use it for a preliminary exploration of the parameter space, searching for the more promising regions to be undertaken by computer simulation means. In order to perform this task, alternative closures to HNC could be employed,[45,46] and density functional theory schemes may be also considered instead of the integral equation approach for the calculation of the PMFs.[13,47]

With regard to the specific details of the model system and computer simulation techniques under consideration, some further comments are deserving. The use of soft-sphere core potentials allows a straightforward calculation of the net (direct plus mediated) forces between the two nanoparticles through the use of Eqs. (4) and (5), thus facilitating substantially the task of calculating the corresponding effective interactions in comparison to an equivalent model system but with hard-sphere cores instead.[15] On the other hand, a fundamental hypothesis of the P-A Ewald approach is the homogeneity of the Coulombic system. Hence, it is remarkable that the good agreement displayed with respect to the standard Ewald summation method even in systems with some degree of anisotropy. Furthermore, the P-A Ewald technique has the extra virtue of being very efficient for a small to sizable number of particles in GPUs,[30] thus allowing faster calculations. These advantages should be profitable when extending this line of inquire to more sophisticated models which may include charge images,[48] molecular electrolytes,[49] ionic solubility,[50] etc.

ACKNOWLEDGMENTS

G. I. G.-G. thanks Prateek Kumar Jha and Rastko Sknepnek for their kind help to use GPUs in MD simulations. The authors thank William Kung for proof-reading our manuscript. MD simulations were in part performed on Quest cluster at Northwestern University. A part of GPU simulations presented in this work were executed on GTX 480 GPUs provided by NVIDIA through their Professor Partnership Program. This material is based upon work supported by the Office of the Director of Defense Research and Engineering (DDR&E) and the Air Force Office of Scientific Research (AFOSR) under Award No. FA9550-10-1-0167, the National Science Foundation (NSF) grant (Grant No. DMR-0520513) of the Materials Research Science and Engineering Center program at Northwestern University and by the Conacyt-México grant (Grant No. 152532).

[1] F. Fenell-Evans and H. Wennerström, *The Colloidal Domain: Where Physics, Chemistry, Biology and Technology Meet* (Wiley-VCH, New York, 1994).
[2] P. C. Hiemenz and R. Rajagopalan, *Principles of Colloid and Surface Chemistry* (Marcel Dekker, New York, 1997).
[3] D. A. Walker, B. Kowalczyk, M. Olvera de la Cruz, and B. A. Grzybowski, Nanoscale **3**, 1316 (2011).
[4] M. Quesada-Pérez, E. González-Tovar, A. Martín-Molina, M. Lozada-Cassou, and R. Hidalgo-Álvarez, Colloids Surf., A **267**, 24 (2005).
[5] C. Schneider, M. Hanisch, B. Wedel, A. Jusuï, and M. Ballauff, J. Colloid Interface Sci. **358**, 62 (2011).
[6] K. Besteman, M. A. G. Zevenbergen, H. A. Heering, and S. G. Lemay, Phys. Rev. Lett. **93**, 170802 (2004).
[7] F. H. J. van der Heyden, D. Stein, K. Besteman, S. G. Lemay, and C. Dekker, Phys. Rev. Lett. **96**, 224502 (2006).
[8] E. Raspaud, M. Olvera de la Cruz, J. L. Sikorav, and F. Livolant, Biophys. J. **74**, 381 (1998).
[9] E. Raspaud, I. Chaperon, A. Leforestier, and F. Livolant, Biophys. J. **77**, 1547 (1999).
[10] E. González-Tovar, F. Jiménez-Angeles, R. Messina, and M. Lozada-Cassou, J. Chem. Phys. **120**, 9782 (2004).
[11] A. P. dos Santos, A. Diehl, and Y. Levin, J. Chem. Phys. **130**, 124110 (2009).
[12] A. P. dos Santos, A. Diehl, and Y. Levin, J. Chem. Phys. **132**, 104105 (2010).
[13] C. N. Patra, J. Phys. Chem. B **114**, 10550 (2010).
[14] B. Modak, C. N. Patra, S. K. Ghosh, and J. Vijayasundar, Mol. Phys. **109**, 639 (2011).
[15] J. Z. Wu, D. Bratko, H. W. Blanch, and J. M. Prausnitz, J. Chem. Phys. **111**, 7084 (1999).
[16] W. Kung, P. González-Mozuelos, and M. Olvera de la Cruz, Soft Matter **6**, 331 (2010).
[17] G. I. Guerrero-García, E. González-Tovar, and M. Olvera de la Cruz, Soft Matter **6**, 2056 (2010).
[18] K. J. M. Bishop and B. A. Grzybowski, ChemPhysChem **8**, 2171 (2007); K. J. M. Bishop, B. Kowalczyk, and B. A. Grzybowski, J. Phys. Chem.

B **113**, 1413 (2009); D. Wang, B. Tejerina, I. Lagzi, B. Kowalczyk, and B. A. Grzybowski, ACS Nano **5**, 530 (2011).
[19]T. Laaksonen, P. Ahonen, C. Johans, and K. Kontturi, ChemPhysChem **7**, 2143 (2006).
[20]B. Lu and A. R. Denton, Phys. Rev. E **75**, 061403 (2007); A. P. Hynninen and A. Z. Panagiotopoulos, J. Phys.: Condens. Matter **21**, 465104 (2009).
[21]M. O. Robbins, K. Kremer, and G. S. Grest, J. Chem. Phys. **88**, 3286 (1988); S. Hamaguchi, R. T. Farouki, and D. H. E. Dubin, Phys. Rev. E **56**, 4671 (1997); F. Sciortino, S. Mossa, E. Zaccarelli, and P. Tartaglia, Phys. Rev. Lett. **93**, 055701 (2004); D. Zhang, P. González-Mozuelos, and M. Olvera de la Cruz, J. Phys. Chem. C **114**, 3754 (2010).
[22]E. González-Tovar, Mol. Phys. **97**, 1203 (1999); Q. Yan and J. J. de Pablo, Phys. Rev. Lett. **86**, 2054 (2001); J. Reščič and P. Linse, J. Chem. Phys. **114**, 10131 (2001); Q. Yan and J. J. de Pablo, Phys. Rev. Lett. **88**, 095504 (2002); A. Z. Panagiotopoulos and M. E. Fisher, *ibid* **88**, 045701 (2002); A. P. Hynninen, M. Dijkstra, and A. Z. Panagiotopoulos, J. Chem. Phys. **123**, 084903 (2005).
[23]W. Kung, F. J. Solis, and M. Olvera de la Cruz, J. Chem. Phys. **130**, 044502 (2009).
[24]J. Zwanikken and R. van Roij, Phys. Rev. Lett. **99**, 178301 (2007).
[25]M. P. Allen and D. J. Tildesley, *Computer Simulation of Liquids* (Clarendon, Oxford, 1987).
[26]R. W. Hockney and J. W. Eastwood, *Computer Simulation Using Particles* (McGraw-Hill, New York, 1981); T. Darden, D. York, and L. Pedersen, J. Chem. Phys. **98**, 10089 (1993); U. Essmann, L. Perera, M. L. Berkowitz, T. Darden, H. Lee, and L. G. Pedersen, J. Chem. Phys. **103**, 8577 (1995).
[27]J. A. Anderson, C. D. Lorenz, and A. Travesset, J. Comput. Phys. **227**, 5342 (2008).
[28]P. Guo, R. Sknepnek, and M. Olvera de la Cruz, J. Phys. Chem. C **115**, 6484 (2011).
[29]E. Yakub and C. Ronchi, J. Chem. Phys. **119**, 11556 (2003); E. Yakub and C. Ronchi, J. Low Temp. Phys. **139**, 633 (2005); E. Yakub, J. Phys. A **39**, 4643 (2006).
[30]P. K. Jha, R. Sknepnek, G. I. Guerrero-García, and M. Olvera de la Cruz, J. Chem. Theory Comput. **6**, 3058 (2010).
[31]D. Wolf, P. Keblinski, S. R. Phillpot, and J. Eggebrecht, J. Chem. Phys. **110**, 8254 (1999); D. Zahn, B. Schilling, and S. M. Kast, J. Phys. Chem. B **106**, 10725 (2002); C. J. Fennell and J. D. Gezelter, J. Chem. Phys. **124**, 234104 (2006); C. Avendaño and A. Gil-Villegas, Mol. Phys. **104**, 1475 (2006); G. Jiménez-Serratos, C. Avendaño, A. Gil-Villegas, and E. González-Tovar, *ibid* **109**, 27 (2011).
[32]I. Fukuda, Y. Yonezawa, and H. Nakamura, J. Chem. Phys. **134**, 164107 (2011).
[33]HOOMD Blue, see http://codeblue.umich.edu/hoomd-blue/ (August 20, 2010).
[34]S. Plimpton, J. Comput. Phys. **117**, 1 (1995).
[35]LAMMPS Molecular Dynamics Simulator, see http://lammps.sandia.gov/ (August 20, 2010).
[36]S. Nosé, Mol. Phys. **52**, 255 (1984).
[37]W. G. Hoover, Phys. Rev. A **31**, 1695 (1985).
[38]K.-C. Ng, J. Chem. Phys. **61**, 2680 (1974).
[39]P. González-Mozuelos and M. D. Carbajal-Tinoco, J. Chem. Phys. **109**, 11074 (1998).
[40]W. B. Russel, D. A. Saville, and W. R. Schowalter, *Colloidal Dispersions* (Cambridge University Press, Cambridge, England, 1989).
[41]L. F. Rojas-Ochoa, R. Castañeda-Priego, V. Lobaskin, A. Stradner, F. Scheffold, and P. Schurtenberger, Phys. Rev. Lett. **100**, 178304 (2008).
[42]M. Peláez-Fernández, A. Moncho-Jordá, and J. Callejas-Fernández, Europhys. Lett. **90**, 46005 (2010).
[43]G. I. Guerrero-García, E. González-Tovar, and M. Olvera de la Cruz, J. Chem. Phys. **135**, 054701 (2011).
[44]T. E. Colla, Y. Levin, and E. Trizac, J. Chem. Phys. **131**, 074115 (2009); T. E. Colla and Y. Levin, J. Chem. Phys. **133**, 234105 (2010); J. M. Falcón-González and R. Castañeda-Priego, Phys. Rev. E **83**, 041401 (2011).
[45]M. D. Carbajal-Tinoco and P. González-Mozuelos, J. Chem. Phys. **117**, 2344 (2002).
[46]J. W. Zwanikken, P. K. Jha, and M. Olvera de la Cruz, J. Chem. Phys. **135**, 064106 (2011).
[47]J. W. Zwanikken and M. Olvera de la Cruz, Phys. Rev. E **82**, 050401 (2010).
[48]A. P. dos Santos, A. Bakhshandeh, and Y. Levin, J. Chem. Phys. **135**, 044124 (2011); A. Bakhshandeh, A. P. dos Santos, and Y. Levin, Phys. Rev. Lett. **107**, 107801 (2011).
[49]P. González-Mozuelos, M. S. Yeom, and M. Olvera de la Cruz, Eur. Phys. J. E **16**, 167 (2005).
[50]P. González-Mozuelos, J. Phys. Chem. B **110**, 22702 (2006).